Effect of Biochar on Transformation of Dissolved Organic Matter and DTPA-Extractable Cu and Cd During Sediment Composting

Meihua Zhao
Guangzhou University
Caiyuan Cai
Guangzhou University
Zhen Yu (yuzhen@soil.gd.cn)
Guangdong Institute of Eco-Environmental and Soil Sciences
Hongwei Rong
Guangzhou University
Chaosheng Zhang
Guangzhou University
Shungui Zhou
Guangdong Institute of Eco-Environmental and Soil Sciences

Research Article

Keywords: sediment, composting, biochar, DOM, heavy metals.

Posted Date: March 3rd, 2021

DOI: https://doi.org/10.21203/rs.3.rs-246796/v1

Version of Record: A version of this preprint was published at Environmental Science and Pollution Research on January 4th, 2022. See the published version at https://doi.org/10.1007/s11356-021-14255-0.

Effect of biochar on transformation of dissolved organic matter and DTPA-extractable Cu and Cd during sediment composting

Meihua Zhao[a,b], Caiyuan Cai[a], Zhen Yu[c,*], Hongwei Rong[a], Chaosheng Zhang[a], Shungui Zhou[c]

[a] School of Civil Engineering, Guangzhou University, Guangzhou 510006, China

[b] National and Local Joint Engineering Laboratory for Municipal Sewage Resource Utilization Technology, Suzhou University of Science and Technology, Suzhou 215009, China

[c] National-Regional Joint Engineering Research Center for Soil Pollution Control and Remediation in South China, Guangdong Key Laboratory of Integrated Agro-environmental Pollution Control and Management, Institute of Eco-environmental and Soil Sciences, Guangdong Academy of Sciences, Guangzhou 510650, China

Abstract:

This study investigated the influence of biochar on temperature, pH, organic matter (OM), seed germination (GI), the fluorescent components of dissolved organic matter (DOM), and bioavailability of DTPA-extractable Cu and Cd during composting and analyzed the relation between DTPA-extractable metals with pH, OM, and the fluorescent components of DOM. Results showed that the addition of biochar shortened the thermophilic phase, reduced the pH at maturation period, accelerated the decomposition of OM, and raised GI. Besides, it promoted the formation of components with benzene ring in FA and HyI and the degradation of protein-like

*Corresponding author at: Institute of Eco-environmental and Soil Sciences, Guangdong Academy of Sciences, Guangzhou 510650, China. E-mail address: yuzhen@soil.gd.cn (Z. Yu).

organic-matters in FA and HA, which was mainly related with the decrease of DTPA-extractable Cd and the increase of DTPA-extractable Cu. After composting, DTPA-extractable Cd in pile A and pile B were decreased by 37.15% and 27.54%, respectively, while the bioavailability of Cu in pile A and pile B were increased by 65.71% and 68.70%, respectively. All these findings demonstrate positive and negative impact produced by biochar into various heavy metals and the necessary of optimization measures with biochar in sediment composting.

Key words: sediment, composting, biochar, DOM, heavy metals.

1. Introduction

Sediment, the primary repository and sink for contaminants in water, is an inseparable part of aquatic ecosystems. The sediment would be contaminated severely by trace metals because of heavy metals pollution in water. The heavy metals stored in river sediments can be released into the overlying water when the environmental conditions varied (Chen et al. 2017, Yi, Yang and Zhang 2011). Therefore, sediment becomes both carrier and potential sources for heavy metals in aquatic environment, which has aroused worldwide concern (Lasheen and Ammar 2016).

Composting is a relatively simple, economical and practical *ex-situ* remediation technology for sediment. Although the total content of heavy metals cannot be decreased, the bioavailability of heavy metals would be reduced after composting (Walter, Martinez and Cala 2006). To enhance the performance of composting, varieties of additives were used, such as biochar (Liu et al. 2017) and zeolite (Singh and Kalamdhad 2015), *Phanerochaete chrysosporium* (Chen et al. 2019). These additives can improve the efficiency of the passivation of heavy metals during composting, then decreasing the toxicity and mobility of heavy metals. Diethylene triamine penta-acetic acid (DTPA)-extractable metal represent a chemical method wildly used to check the plant available fraction in soils, sludge-amended soils, and sludge composting products (Katyal and Sharma 1991, Fang and Wong 1999).

Biochar is a porous, carbonaceous product obtained from the pyrolysis of organic materials such as sludges, plant materials and manures (Paz-Ferreiro et al. 2014). Paz-Ferreiro et al. (2014) also reviewed that biochar was widely used to remediate

soils contaminated by heavy metals because of its high cation exchange capacity and many potential benefits. At the same time, there are some studies on the bioavailability of heavy metals from composting adding biochar have been reported (Chen et al. 2017, Liang et al. 2017). These reports showed that biochar effectively reduced the mobility and availability of heavy metals during composting process. pH and organic matter (OM) play an important role in passivating heavy metals during composting process and they would affect the heavy metals accumulated by both plants and animals (Li et al. 2010). The dissolved organic matter (DOM) can be fractioned into fulvic acids (FA), humic acids (HA), and hydrophilic (HyI) fractions and it was the main material affecting the active of heavy metals (He et al. 2019). The evolution information and the composition of DOM could be successfully observed through the excitation emission matrix (EEM) in combination with parallel factor analysis (PARAFAC) (Yuan et al. 2017, Zhao et al. 2017, Cory and McKnight 2005). However, most previous studies had only focused on the FA and HA fractions, but neglected the HyI fraction. Besides, the research of taking the influence of biochar on the pH, OM, the fluorescent components of DOM and the toxicity of heavy metals during composting of river sediment into consideration was limited. Therefore, it is significant to carry out such study to detect the effect of biochar on the fluorescent components of DOM. Besides, analyzing the correlation between bioavailable heavy metals with pH and OM, and the fluorescent components of DOM during composting is also conducive to understand the mechanism of passivation of heavy metals in composting of sediment.

This study was aimed to evaluate the influence of biochar on the bioavailability of Cu and Cd (extraction with DTPA) and the fluorescent components of FA, HA, and HyI during composting process of river sediment. Meanwhile, variations of parameters such as temperature, pH, OM loss and germination index (GI) during composting process were investigated. Moreover, the correlation between the DTPA-extractable metals (Cu and Cd) with pH, OM and the fluorescent components of FA, HA, and HyI were also analyzed. Some valuable information for biochar affecting the passivation of heavy metals in composting of sediment contaminated by heavy metals is expected to provide in this research.

2. Materials and methods

2.1 Composting materials

In this experiment, the sediment was collected from the surface layer (0-20 cm) of the river in Shao Guan City, Guang Dong Province and was shipped back to the laboratory with clean containers. The sediment was air-dried at room temperature, following removing impurities such as roots, leaves, and gravel, grinding and passing through a sieve with a pore size of 1.0 cm. The air-dried rice straw with the length of about 1-2 cm was purchased from Jining city, Shandong Province and used as organic substances hard to be biodegradable (Zeng et al. 2009). Bran was used for adjusting the initial C/N of composting. Several kinds of vegetable chopped up into small pieces were used as easily biodegradable organic matter. Biochar was formed from pine wood flakes by cracking at 500 ℃ in carbonation furnace for 30 min. After

cooling to room temperature, ground and sieved it through an 80-mesh sieve. The basic physicochemical properties of these raw materials are shown in Table 1.

Table 1 The basic physicochemical properties of the composting raw materials.

item	Moisture content（%）	pH	TOC（g/kg）	TN（g/kg）	C/N
Sediment	18.58	4.76	61.98	4.25	14.59
Rice straw	12.95	6.88	674.84	9.68	62.46
Bran	13.22	6.58	696.85	24.74	26.12
Vegetable	94.93	7.75	457.52	33.30	13.74
Biochar	4.12	6.65	-	-	-

"-", no detection.

TOC, total organic carbon.

TN, total nitrogen.

C/N, TOC/TN.

2.2 Composting design and sample collection

There were two co-composting systems in this experiment, corresponding pile A and pile B. Pile A was the control group while the pile B was added with 10% biochar (Kim et al. 2015). Before adding the biochar, the initial moisture content and C/N of these two piles were about 55% and 32, respectively. The ratio of sediment, straw, bran and vegetable was about 13:4:2:1 (w/w/w/w). The two composting materials approximately 20 kg (moist weight) were mixed homogenizedly and loosely packed in the same polypropylene container which has dimension of 63cm×45cm×38cm (length × width × height). To prevent anaerobic conditions, the mixture was manually

111 turned twice a week in the first two weeks and then once a week until the termination
112 of composting (Zeng et al. 2009). What's more, the study was carried out under room
113 temperature and pH natural conditions.

114 Recorded the day when the heaps were finished as day 0. The composting
115 process lasted for 60 days. Samples were taken from the heap using five different
116 sampling methods according to Chen et al. (2017) at 10 am at day 0、2、4、8、12、
117 20、36、45 and 60, then mixing fully and dividing into two parts. One part was used
118 for the determination of pH and OM. One part was air-dried to measure heavy metals
119 after grounding and sieving through 100-mesh sieve. The remaining part was stored at
120 -20 ℃ for further analysis. Temperatures were recorded at 10 am and 4 pm by reading
121 the value of thermometer inserting into the center of pile, following taking the average
122 value. The ambient temperature was also recorded with the same specification
123 thermometer. In addition, the samples at the day 0, 4, 12, 36, and 60 were used to
124 measure the GI values and extract the HA, FA and HyI fractions.

125 **2.3 Parameter analytical methods**

126 pH values were determined according to the method reported by Zeng et al.
127 (2007). The ash content was measured by fresh sample drying at 105±2 ℃ for 6-8 h
128 and then igniting in muffle furnace at 550±2 ℃ for 8 h. The OM was calculated by
129 ash content. The GI was measured according to the method reported by Zhou et al.
130 (2018).

131 The HA, FA and HyI fractions were extracted and purified according to the
132 method of He et al. (2019). Prepared 0.1 mol/L NaOH solution and 0.1 mol/L

133 $Na_4P_2O_7$ solution, respectively, and mixed them according to volume ratio of 1:1.
134 The mixed solution was taken according to dry sample-liquid ratio of 10:1 to dissolve
135 the sample, then mechanical shock was carried out in nitrogen environment with a
136 constant temperature of 20 ℃ for 24 h. The pH of the shaken solution was adjusted to
137 1 with 6 mol/L HCl solution, and then centrifuged at 10000 rpm. After centrifugation,
138 the HA, FA and HyI fractions were separated. The precipitate was HA, the
139 supernatant was FA and Hyl. The HA (precipitate) was dissolved again in 0.1 mol/L
140 NaOH solution and centrifuged at 10000 rpm. Collected the supernatant, which was
141 acidified to pH=1.5 and then centrifuged. Rinsed the HA with ultrapure water until all
142 the Cl^- has eliminated. The separation of FA and Hyl containing in supernatants above
143 was used XAD-8 column. The FA fraction was adsorbed by XAD-8 column and the
144 Hyl fraction was pass through XAD-8 column. The FA on the column was eluted with
145 0.1 mol/L NaOH. In addition, to remove the cations, purified the FA was purified
146 with hydrogen cation exchange resin. What's more, further purified the Hyl fraction
147 with hydrogen type cation exchange resin to remove the cations.

148 The F-7000 fluorescence spectrophotometer (Hitachi, Japan) was used to
149 measure the EEM fluorescence spectra according to the method of He et al. (2019).
150 However, adjusted the dissolved organic carbon of the samples to 10 mg/L before
151 spectral analysis. The analysis of fluorescence data set was used PARAFAC
152 DOMFluor toolbox in Matlab 2015. The maximum fluorescence intensity (F_{max})
153 value, acquiring through PARAFAC analysis, was represented the relative content of
154 certain component in the sample.

155 The total concentration of heavy metals (Cu and Cd) was determined through
156 ICP-OES after digesting the sample (0.2500 g, air-dried, sieved through 10 mesh
157 nylon sieve) with $HClO_4$: HF: HNO_3. The concentrations of DTPA-extractable Cu
158 and Cd were acquired by mechanically shaking 3.0 g air-dried sample (sieved to < 2
159 mm) with 20 mL of 0.005 mol/L DTPA extracts (0.005mol/L DTPA + 0.01mol/L
160 $CaCl_2$ + 0.1mol/L triethanolamine, buffered to pH 7.30 using hydrochloric acid
161 solution or ammonia). After oscillating, centrifuged and filtrated with 0.45 μm filter
162 membrane immediately. Retained the filtrate and finished detecting within 48 h.
163 For getting more accurate results, all composting samples were processed in
164 triplicates and the results are showed as mean ± standard deviations (S.D.).

165 **2.4 Data processing and statistical analysis**

166 The OM losses were calculated using the following equation (Zhao et al. 2016,
167 Dias et al. 2010, Serramia et al. 2010):

168 $$OM_{loss} = 100 \times \left[1 - \frac{X_0 (100 - X_1)}{X_1 (100 - X_0)} \right]$$

169 Where, X_0 : initial ash content (%); X_1 : final ash content (%).

170 The equation calculated the extraction efficiency of DTPA-extractable heavy
171 metal was shown below (Chen et al. 2010) :

172 $$Extraction\ efficiency\ (\%) = \frac{C_{DTPA-HM}}{C_{Total-HM}} \times 100$$

173 Where $C_{DTAP-HM}$ and $C_{Total-HM}$ are the concentration of DTPA-extractable
174 heavy metal and the total concentration of heavy metal, respectively.

175 Origin 8.5 and matalb were conducted to plot figures, and the SPSS 16.0

176 software was used for multivariate statistical analysis.

177 **3. Results and discussion**

178 **3.1 Variation of physicochemical parameters during composting**

179 Fig. 1 exhibited the temperature change, while Table 2 showed the variation of
180 pH, OM, OM loss and GI values of both pile during composting process. Temperature
181 is one of the most important parameters which reflects the dynamic process of
182 microbial growth and organic degradation during composting (Yu et al. 2018, Zhang
183 et al. 2018). Both piles showed a rapidly increase of temperature during the first day,
184 following by achieving the thermophilic temperatures (T > 55 °C) on the second day
185 and reaching up to the temperature maximum on the fourth day. This might attribute
186 to the rapid degradation of organic matter by micro-organism at the early stage of the
187 composting process (Awasthi et al. 2016, Ren et al. 2010). However, compare with
188 pile A, pile B performed a shorter duration of thermophilic phase. The thermophilic
189 phase of pile A lasted 8 days while that of pile B only maintained for 6 days. Then the
190 temperatures of both trials decreased gradually to or close to ambient temperature.
191 This result was opposite to previous observations that biochar addition to composting
192 exerted a positive effect on trial temperature (Chen et al. 2017, Jindo et al. 2012,
193 Sanchez-Garcia et al. 2015). This change might be explained that the biochar
194 composed of pine wood flakes at 500 °C produced negative excitation effect on the
195 decomposition of native organic carbon of trail, then influencing the temperature of
196 trial added with biochar (Jones et al. 2011).

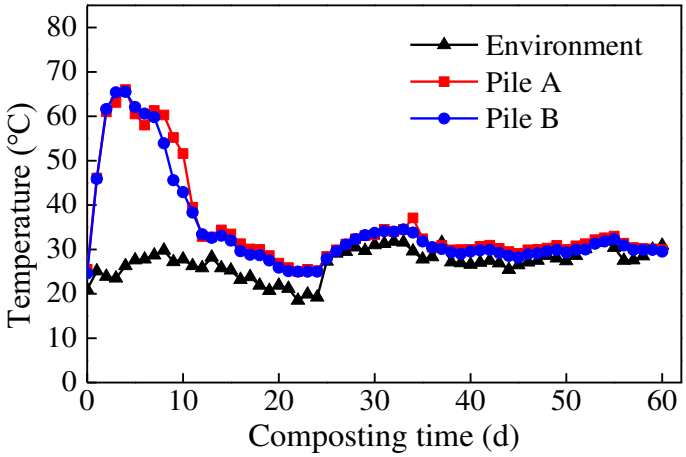

Fig. 1 The temperature diagram during composting process.

Table 2 The dynamics of physicochemical parameters during 60-day composting.

Parameters	Day	pH	OM (g/kg)	OM loss (%)	GI (%)
Pile A	0	5.31 (0.03)	425.89 (13.56)	0	50.49 (0.07)
	2	5.86 (0.04)	425.44 (13.38)	8.80 (1.64)	
	4	6.18 (0.04)	393.73 (2.95)	16.84 (1.28)	62.70 (0.05)
	8	7.48 (0.05)	365.27 (19.36)	28.58 (1.37)	
	12	7.49 (0.04)	349.64 (18.38)	31.13 (4.47)	66.33 (0.03)
	20	7.45 (0.02)	346.96 (3.78）	31.97 (1.18)	
	28	7.40 (0.03)	335.45 (6.64)	32.67 (1.55)	
	36	7.37 (0.02)	321.14 (1.72)	33.93 (5.46)	57.98 (0.09)
	45	7.39 (0.04)	335.41 (11.56)	34.07 (1.71)	
	60	7.26 (0.07)	327.80 (17.03)	34.34 (1.47)	68.30 (0.07)
Pile B	0	5.60 (0.10)	430.83 (9.95)	0	69.65 (0.04)
	2	6.43 (0.12)	401.28 (14.58)	14.63 (3.11)	
	4	6.81 (0.07)	378.77 (13.92)	22.80 (2.31)	63.96 (0.06)
	8	7.52 (0.04)	340.45 (15.94)	31.74 (3.35)	
	12	7.40 (0.02)	321.12 (6.82)	37.77 (0.80)	81.89 (0.04)
	20	7.38 (0.04)	344.48 (16.29)	35.82 (4.63)	
	28	7.34 (0.02)	334.53 (20.13)	38.55 (5.55)	
	36	6.56 (0.04)	333.59 (11.46)	38.09 (2.43)	111.58 (0.01)
	45	6.38 (0.09)	322.73 (15.04)	41.73 (4.04)	
	60	6.67 (0.05)	319.57 (10.84)	42.75 (2.00)	102.35 (0.08)

The numeral in brackets stands for is standard for deviation, n=3.

pH is another important factor affecting the microbial activity and composting process. Chen and Yong (2012) reported that aerobic composting can be done with pH between 5 and 9. Therefore, this composting was conducted without adjusting the pH of raw composting materials. The initial pH of pile B was slightly greater than the control group due to the dilution of biochar. At early stage of composting, the pH of pile A increased rapidly and turned to reach a maximum (7.49) at day 8 while pile B got a maximum (7.52) at day 6. Then the pH of pile A only had a slight drop (from 7.49-7.26) until the end of composting. However, the pH in pile B was sharply decreased from day 12-day 45, getting the minimum value of pH at day 45, then slightly increased and reached 6.67 at the end of the composting. According to Meng et al. (2019), the rapid increase in the pH of both piles might be related to denitrification which indicated that the release rate of ammonia was much higher than the fixed rate of nitrogen nitrate during the early time of composting process, thus increasing the pH in both two trails significantly. A sudden drop of pH in pile B from day 12-day 45 may be due to the sharp reduction of ammonia volatilization rate and the enhancement of nitrification at the late stage of composting (Meng et al. 2019). Besides, the decrease of pH in pile B from day 12-day 45 may also be related to the ability of biochar to absorb cations (Zhang et al. 2016). pH of the compost products of both piles was within the suitable pH for seed growth (6.5-7.5) (Zhang and Sun 2017).

The degradation and mineralization process during aerobic composting were exhibited by the reduction of OM (Chen et al. 2017, Zhao et al. 2016). At the same

223 time, the OM loss can be used to estimate the OM degradation during composting
224 process. Generally, the OM loss of both piles increased during composting process.
225 The increase rate of OM loss at the early stage was higher than that at the end of
226 composting mainly because of the reduction of easily biodegradable organic
227 compounds in composting raw materials as well as the synthesis reactions of new
228 complex and polymerized organic matter during the maturation phase (Zhao et al.
229 2016). The increase rate of OM loss in pile B was higher than that of pile A during the
230 composting process, indicating the intense OM decomposition in trial with biochar.
231 Sanchez-Garcia et al. (2015) pointed that biochar with high porosity can accelerate
232 the degradation of OM by improving aeration conditions and promoting microbial
233 metabolism in composting.

234 Previous reports pointed out that the GI based on relative seed germination
235 number and relative root length is considered as the most important biological
236 indicator to evaluate the toxicity and maturity of compost products (Barje et al. 2013,
237 Chan Selvam and Wong 2016, Awasthi et al. 2015). When GI value is greater than
238 80%, the plant toxicity of composting products is lower and the maturity degree is
239 better; when GI value is less than 80%, the plant toxicity in composting products is
240 higher and the maturity degree is more insufficient (Rashad, Saleh and Moselhy 2010,
241 Ranalli et al. 2001). Table 2 showed the obvious changes in GI values during
242 composting process. After a decrease in the first 4 days, GI of pile B increased
243 observably, then reaching and over 80% at around 12 to 60 days, whose compost
244 products could be considered as non-phytotoxic (Riffaldi et al. 1986). The GI of pile

A increased during first the 12 days, but had a slow decrease from day 12 to day 36 and a slight decrease until the end of the composting. At the end of composting, the GI value of pile B (102.35%) was greater than that of pile A (68.30%), which revealed that the toxicity of compost products to plants weakened due to the addition of biochar.

3.2 The fluorescent components of the DOM and their changes during composting process

Three fluorescent components were identified from HA, FA and HyI fractions by PARAFAC model (Fig. 2). These fluorescent components have many similarities with the fluorescence peaks identified in previous studies. Component 1 (C1) had an excitation wavelength at 315 nm and an emission wavelength at 415 nm. He et al. (2019) also found a similar peak in the compost of municipal solid waste and considered it as benzene substances. Component 2 (C2) exhibited two obvious excitation peaks at 265 nm and 330 nm, and its largest emission peak at 475 nm, which is similar to the fluorescence spectra of quinone compounds (Cory and McKnight 2005). Component 3 (C3) (E_x/E_m = 225, 275/350**Error! Reference source not found.**) had two fluorescence peaks, resulting by the interaction between tyrosin-like and tryptophan-like proteins (Chen et al. 2003, Yao et al. 2011).

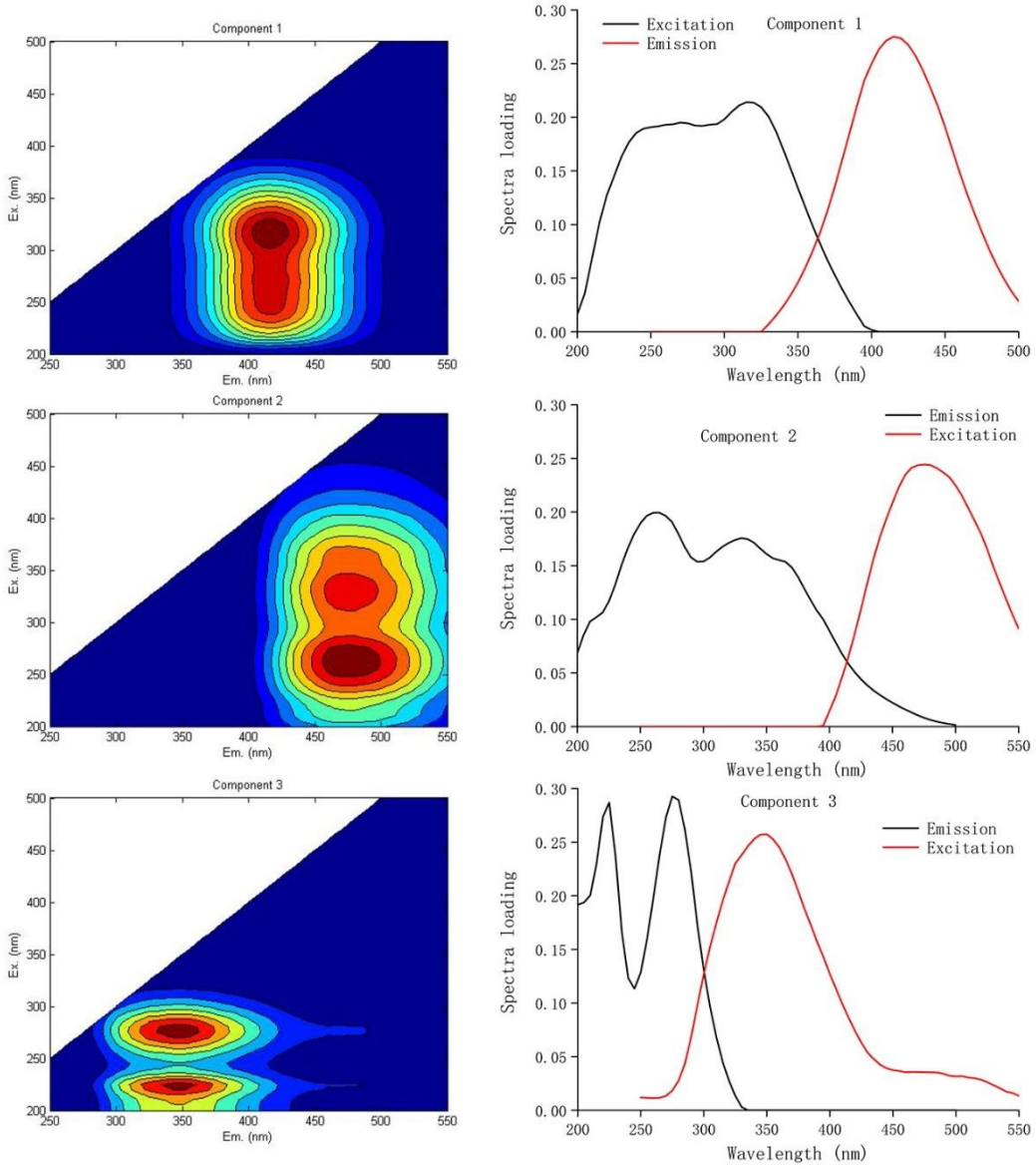

Fig. 2 Three fluorescent components identified by PARAFAC model and their loadings.

The fluorescence intensity can be used to indirectly reveal the changes of fluorescent components of DOM because the intrinsic fluorescence of organic components in soil contains information related to structural components, functional groups, conformation and heterogeneity, as well as the dynamic characteristics of their intramolecular/intermolecular interactions (D'Orazio, Traversa and Senesi 2013). Fig.3 showed the evolution of the F_{max} of different fluorescent components of FA (a,

272 b), HA (c, d), and HyI (e, f) at different composting stages. For FA (Fig. 3 a, b), we
273 can see that the variation trends of F_{max} of C3 of both piles were decreased with
274 increasing composting time. The F_{max} of C1 increased from the original 1427.21
275 R.U to 2811.22 R.U while the F_{max} of C2 also increased slowly from 738.73 R.U to
276 1518.07 R.U in pile A. Compared with pile A, the F_{max} of C1 in pile B increased
277 from 1576.60 R.U to 2959.74 R.U within 12 days and stayed there for some time,
278 then increased to 3318.69 R.U. On the other hand, the F_{max} of C2 increased from
279 767.52 R.U to 1577.91 R.U, and then decreased to 1462.40 R.U during composting
280 process. This phenomenon suggests that biochar can promote the formation of
281 benzene-containing compounds. Besides, it may also contribute to the phenyl
282 structure of biochar. With regard to HA (Fig. 2 c, d), the F_{max} of C3 in both trials
283 decreased during the composting process, indicating that the relative content of
284 protein of HA in both piles was also decreasing. At the same time, the F_{max} of C1
285 and C2 of the FA in both trials were enhanced, but the difference of increase was not
286 significant. Notably, the F_{max} of the functional components of HyI are significantly
287 different from those of FA and HA. According to Fig. 2 (e, f), the F_{max} of C1 in pile
288 A increased from 319.83 R.U on day 0 to 455.24 R.U on day 4, and then rapidly
289 increased to 898.43 R.U on day 36, and finally decreased slightly on day 60. In
290 addition, the F_{max} of C2 in the control group increased slightly with composting time,
291 while the F_{max} of C3 fluctuated in 400-500 R.U. The change of the F_{max} of C1 and
292 C2 in the group with biochar was similar to that in the control group. Compared with
293 the control group, the variation of F_{max} of C3 in the biochar group was more obvious:

the change of the F_{max} of C3 in the early stage of composting was similar to that in the control group, but it was mutated to 601.92 R.U on day 60 of composting, which might be because the aromatic polycondensation or conjugated color groups contained in the protein substances of pile B increased in the later stage of composting (Mayer, Schick and Loder III 1999).

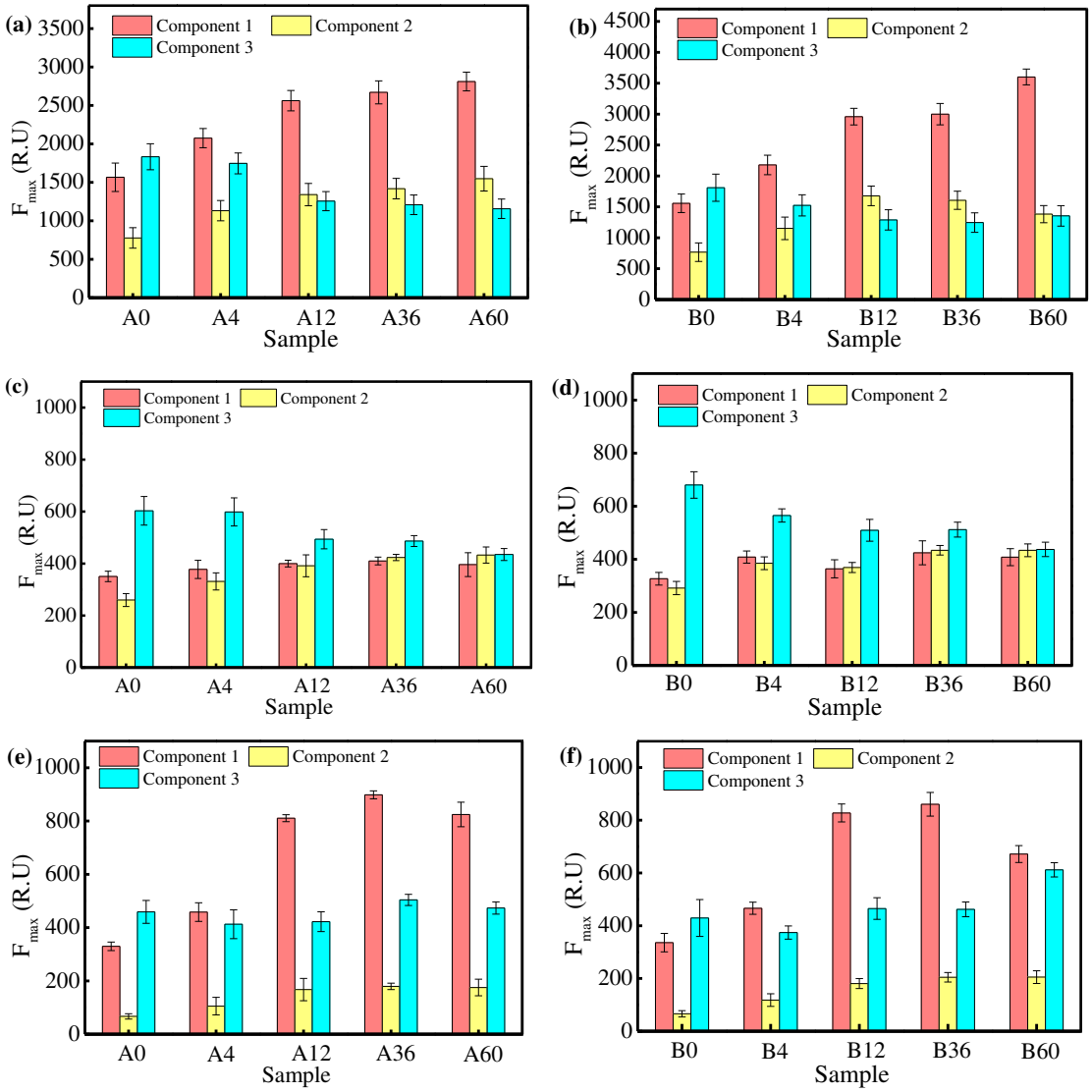

Fig. 3 The evolution of the F_{max} of different fluorescent components of FA (a, b), HA (c, d) and HyI (e, f) during composting.

A0, A4, A12, A36, and A60 respected day 0, 4, 12, 36, and 60 of pile A, respectively;

306 B0, B4, B12, B36, and B60 respected day 0, 4, 12, 36, and 60 of pile B, respectively.

307 **3.3 Variation of Cu and Cd during composting process**

308 **3.3.1 Total contents of Cu and Cd**

309 The changes in total concentrations of Cu and Cd during composting process
310 were presented in Fig. 4. The initial content of the target heavy metals in each trial
311 was Cu > Cd in the order. After 60-day composting, the total concentrations of Cu
312 and Cd increased in both two piles, which was in agreement with the previous studies
313 (Lazzari et al. 2000, Zhou et al. 2018). The concentrations of heavy metals increased
314 after composting mainly because of the decomposition of OM, the release of carbon
315 dioxide and water, and the reduction of bulk volume after composting, then resulting
316 in the increase of total heavy metal concentration in the trials (Liu et al. 2007, Singh,
317 Das and Kalamdhad 2012, Zorpas et al. 2000). In addition, because of the loss of the
318 soluble heavy metals carried by leachate produced in the composting process and the
319 dilution effect of materials such as rice straw, bran, and biochar added in the heap, the
320 heavy metals content of each trial changes observably and differently.

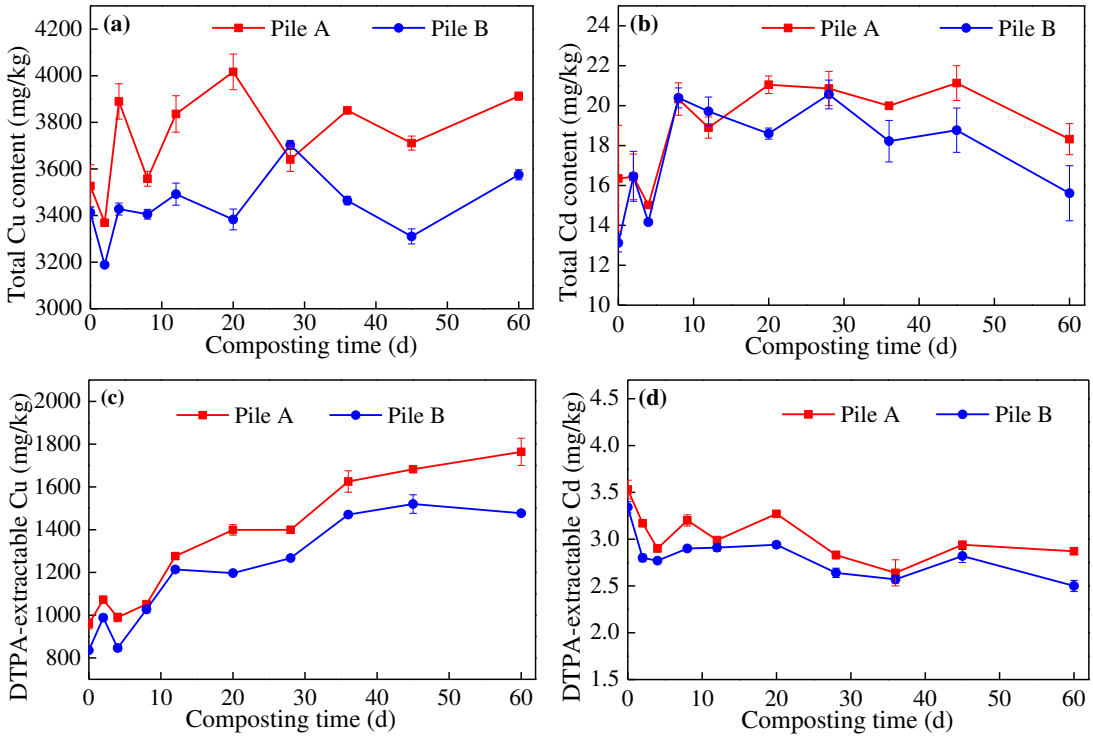

Fig. 4 Changes in contents of total Cu and Cd (a, b), DTPA-extractable Cu and Cd (c, d) during composting process.

3.3.2 Variation of bioavailability of Cu and Cd (extraction with DTPA)

In most cases, it is usual to consider the DTPA-extractable metal contents as a chemical means to estimate the mobility and plant phytotoxicity of heavy metal (Fang and Wong 1999, Chen et al. 2010). As shown in Fig. 4c and d, the DTPA-extractable Cu and Cd contents of both piles changed similarly during composting. Compared with the 0-day stage, the DTPA-extractable Cu contents in both piles increased, which might be related to the dissolution of organic matter during DTPA extraction (Singh

and Kalamdhad 2013). Relative to the 0-day stage, the higher increase (percentage of total Cu) of Cu content was observed in pile B (68.70%) followed by control (65.71%), which means that the biochar enhanced the activity of Cu during composting. Beesley et al. (2010) also found that biochar could enhanced the activity of Cu in soil. However, the DTPA-extractable Cd contents in both piles deceased after composting. The higher reduction of Cd (percentage of total Cd) content in pile A and pile B were about 27.54% and 37.15%, respectively. This result indicated that the addition of biochar to the composting process exerted a positive role in decreasing the plant availability of Cd, which was similar to the results reported by Chen et al. (2017). There were mixed effects on both DTPA-extractable Cu and Cd, the biochar addition to compost enhancing the former but reducing the latter. However，different researchers drawn different conclusions from the morphological changes in heavy metals during composting. For example, Liu et al. (2017) found that the content of available Pb, As, Cu, Cr and Ni decreased but the contents of available Zn and Cd increased after sludge composting. Chen et al. (2010) indicated that the mobility of Cu and Zn reduced during pig manure composting.

3.4 Relationships among the DTPA-extractable Cu and Cd and physicochemical parameters, fluorescent components of the HA, FA and HyI fractions

3.4.1 Pearson correlation between the DTPA-extractable Cu and Cd contents with pH and OM

Table 3 Pearson correlation coefficients of bioavailability of Cu and Cd (DTPA-extractable

357 content) with pH values and OM during 60-day composting for both two piles.

Items	Pile A		Pile B	
	pH	OM	pH	OM
DTPA-extractable Cu	0.661*	-0.855**	0.140	-0.816**
DTPA-extractable Cd	-0.542	0.696*	-0.334	0.646*

358 **Significant correlation at the 0.01 level (bilateral).

359 * Significant correlation at the 0.05 level (bilateral).

360 The correlation coefficients of DTPA-extractable Cu and Cd with pH and OM
361 were studied for determining the effect of pH variation and OM degradation on the
362 plant availability of heavy metals (Table 4). The pH was corelative with the
363 DTPA-extractable Cu in pile A (r = 0.661) while it did not influence the
364 DTPA-extractable Cu in pile B. The pH did not correlate with the DTPA-extractable
365 Cd both in pile A and pile B. The OM significantly correlated with the
366 DTPA-extractable Cu in both pile (r = -0.855 in pile A and r = -0.816, respectively).
367 But the correlation coefficient of pile A was slowly higher than that of pile B. The
368 correlations between DTPA-extractable Cd and OM in both piles were almost the
369 same.

370 The relationship of DTPA-extractable Cu and Cd with OM indicated that the
371 bioavailability of Cu and Cd was significantly influenced by OM degradation during
372 composting process. However, because of the addition of biochar to composting
373 materials (pile B), the relationship of DTPA-extractable Cu with pH and OM was
374 weakened. This result can be explained that biochar with high adsorption capacity for
375 Cu, which disturbed the normal passivation of Cu during composting process.

3.4.2 Relation between the fluorescent components of the DOM and DTPA-extractable Cu and Cd contents

The diagram of the relationship between the fluorescent components of FA, HA, and HyI and the DTPA-extractable concentration of Cu and Cd during the compost process was shown in Fig. 5. Except for the C1 of HyI, the contents of DTPA-extractable Cu were associated with the fluorescent components of the FA, HA, and HyI fractions. Among them, the contents of DTPA-extractable Cu were negatively correlated with the C3 of FA and HA (r = -0.855 and -0.877, respectively). That is to say, the DTPA-extractable Cu increased with the decrease of the content of protein-like substances in fulic acid and humic acid in the pile. However, the contents of DTPA-extractable Cu were positively correlated with the other fluorescent components. As the same time, the contents of DTPA-extractable Cu were mostly positive with C2 of the HA and the C3 of the HyI (r =0.803 and 0.610, respectively). These results indicated that DTPA-extractable Cu were mainly positively correlated with the benzene substances and quinone-like compounds, especially that in the fulic acid and hydrophilic substances. In other words, the content of available Cu (DTPA extraction) increased with the increase of benzene substances and quinone-like compounds in the heap, but benzene substances in HA and quinone-like compounds in HyI were more sensitive to the increase of the activity of Cu, which may be related to the size of the molecular weight contained in DOM. Precious studies found that he components with high molecular weight were more able to reduce the toxicity of Cu (Wang et al., 2010a; Wang et al., 2010b; Tang et al., 2018).

The relationships of DTPA-extractable Cd to the fluorescent components of the FA, HA, and HyI fractions were different from that of the DTPA-extractable Cu. As for the contents of Cd, they were positively correlated with C3 of FA and HA and their correlation coefficients were 0.709 and 0.702, respectively. The negative correlation coefficients of C1 and C2 of FA, C1 and C2 of HA as well as C1, C2 and C3 of HyI were -0.841, -0.755, -0.863, -0.910, -0.672, -0.843, and -0.422, respectively. As mentioned above, the C1 and C2 of FA, HA, and HyI were increased and the C3 of FA, HA, and HyI was decreased at the end of the composting, but the addition of biochar to composting enhanced their variation during the composting. All in all, the decrease of DTPA-extractable Cd was mainly related to the increase of components with benzene-like components in FA and HyI and the decrease of protein-like organic-matters in FA and HA. The addition of biochar to composting may enhance the increase of components with benzene-like substances in FA and HyI and the decrease of protein-like organic-matters in FA and HA during the composting, then reduced the activity of DTPA-extractable Cd.

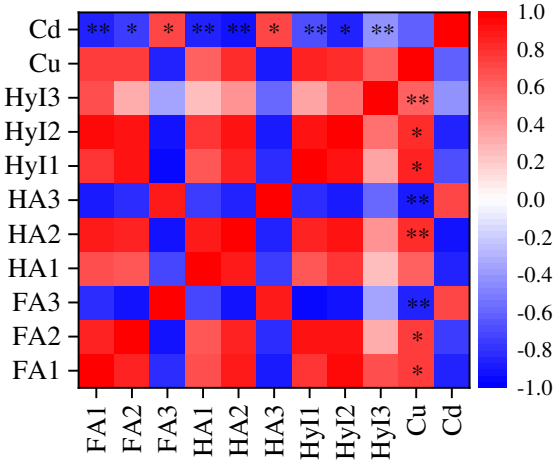

Fig. 5 The diagram of the relationship between the fluorescent components of FA, HA, and HyI

and the DTPA-extractable Cu and Cd contents during the compost process.

FA1, FA2, FA3, HA1, HA2, HA3, HyI1, HyI2, and HyI3 respected the C1, C2, C3 of the FA, the C1, C2, C3 of the HA, and C1, C2, C3 of the HyI, respectively. **, Significant correlation at.01 level (bilateral). *, Significant correlation at the 0.05 level (bilateral).

4. Conclusion

In this study, we compared the composting materials adding with biochar and without biochar during 60-day composting. The results showed that the addition of biochar to composting process affected the variation of temperature, pH, OM, GI, fluorescent components of DOM, and the bioavailability of Cu and Cd. It shortened the thermophilic phase, reduced the pH at the maturation period, increased OM decomposition, and raised the GI of the biochar amended pile. The biochar may promote the formation of benzene-containing compounds in FA and HyI, and the degradation of protein-like organic-matters in FA and HA, which decreased the plant availability of Cd (extraction with DTPA) but increased the plant availability of Cu. Besides, the addition of biochar to composting disturbed the normal passivation of heavy metals during composting process. The bioavailability of Cd (extraction with DTPA) was decreased by 37.15%, while that of control group was only decreased by 27.54%. However, the bioavailability of Cu in pile A and pile B were increased by 65.71% and 68.70%, respectively. What's more, the bioavailability of Cu and Cd were significantly influenced by OM degradation during composting process, but DTPA-extractable Cu and Cd had different relativity with various fluorescent components of FA, HA, and HyI.

CRediT authorship contribution statement

Meihua Zhao: Investigation, Writing-original draft, Funding acquisition. **Caiyuan Cai:** Investigation, Formal analysis, Funding acquisition. **Zhen Yu:** Supervision, Writing-review & editing. **Hongwei Rong:** Data curation, Software, Methodology. **Chaosheng Zhang:** Writing- review & editing, Funding acquisition. **Shungui Zhou:** Writing- review & editing, Visualization. All authors read and approved the manuscript.

Acknowledgements

This study was financially supported by the National Natural Science Foundation of China (51609042, 21477027), the National & Local Joint Engineering Laboratory for Municipal Sewage Resource Utilization Technology, Suzhou University of Science and Technology (2018KF03) and the Basic Innovation Project for Graduate Students of Guangzhou University (2018GDJC-M44).

Declaration of competing interest

The authors declare that they have no known competing financial interests or personal relationships that could have appeared to influence the work reported in this paper.

Ethics approval and consent to participate

Not applicable.

Consent for publication

Not applicable.

Data and materials availability statement

All datasets used and/or analyzed in this study are available from the corresponding author on reasonable request.

461 **References**

462 Awasthi, M. K., Pandey, A. K., Bundela, P. S., & Khan, J., (2015) Co-composting of
463 organic fraction of municipal solid waste mixed with different bulking waste:
464 characterization of physicochemical parameters and microbial enzymatic
465 dynamic. *Bioresour Technol,* 182**,** 200-207.

466 Awasthi, M. K., Pandey, A. K, Bundela, P. S., Wong, J. W. C., Li R., & Zhang, Z.,
467 (2016) Co-composting of gelatin industry sludge combined with organic fraction
468 of municipal solid waste and poultry waste employing zeolite mixed with
469 enriched nitrifying bacterial consortium. *Bioresour Technol,* 213**,** 181-189.

470 Barje, F., El Fels, L., El Hajjouji, H., Winterton, P., & Hafidi, M., (2013)
471 Biodegradation of organic compounds during co-composting of olive oil mill
472 waste and municipal solid waste with added rock phosphate. *Environ Technol,* 34**,**
473 2965-75.

474 Beesley, L., Moreno-Jiménez, E., Gomez-Eyles, J. L., (2010) Effects of biochar and
475 greenwaste compost amendments on mobility, bioavailability and toxicity of
476 inorganic and organic contaminants in amulti-element polluted soil. *Environ.*
477 *Pollut*. 158, 2282–2287.

478 Chan, M. T., Selvam, A., & Wong, J. W., (2016) Reducing nitrogen loss and salinity
479 during 'struvite' food waste composting by zeolite amendment. *Bioresour*
480 *Technol,* 200**,** 838-44.

Chen, W., Westerhoff, P., Leenheer, J. A., & Booksh, K., (2003) Fluorescence excitation-emission matrix regional integration to quantify spectra for dissolved organic matter. *Environ Sci Technol,* 37**,** 5701-10.

Chen, Y., Chen, Y., Li, Y., Wu, Y., Zeng, Z., Xu, R., Wang, S., Li, H., & Zhang, J., (2019) Changes of heavy metal fractions during co-composting of agricultural waste and river sediment with inoculation of Phanerochaete chrysosporium. *J Hazard Mater,* 378**,** 120757.

Chen, Y., Liu, Y., Li, Y., Wu, Y., Chen, Y., Zeng, G., Zhang J., & Li, H., (2017) Influence of biochar on heavy metals and microbial community during composting of river sediment with agricultural wastes. *Bioresour Technol,* 243**,** 347-355.

Chen & Yong (2012) Sewage Sludge Aerobic Composting Technology Research Progress. *Aasri Procedia,* 1**,** 339-343.

Chen, Y. X., Huang, X. D., Han, Z. Y., Huang, X., Hu, B., Shi, D. Z., & Wu, W. X., (2010) Effects of bamboo charcoal and bamboo vinegar on nitrogen conservation and heavy metals immobility during pig manure composting. *Chemosphere,* 78**,** 1177-81.

Cory, R. M. & McKnight, D. M., (2005) Fluorescence spectroscopy reveals ubiquitous presence of oxidized and reduced quinones in dissolved organic matter. *Environ Sci Technol,* 39**,** 8142-9.

501 D'Orazio, V., Traversa, A., & Senesi, N., (2013) Forest Soil Organic Carbon
502 Dynamics as Affected by Plant Species and Their Corresponding Litters: A
503 Fluorescence Spectroscopy Approach. *Plant & Soil,* 374.
504 Dias, B. O., Silva, C. A., Higashikawa, F. S., Roig, A., & Sanchez-Monedero, M. A.,
505 (2010) Use of biochar as bulking agent for the composting of poultry manure:
506 effect on organic matter degradation and humification. *Bioresour Technol,* 101**,**
507 1239-46.
508 Fang, M., & Wong, J. W., (1999) Effects of lime amendment on availability of heavy
509 metals and maturation in sewage sludge composting. *Environ Pollut,* 106**,** 83-9.
510 GILLMAN, G. P., & FOX, R. L., (1980) Increases in the Cation Exchange Capacity of
511 Variable Charge Soils Following Superphosphate Applications1. *Soil Science*
512 *Society of America Journal,* 44**,** 934.
513 He, X. S., Yang, C., You, S. H., Zhang, H., Xi, B. D., Yu, M. D., & Liu, S. J., (2019)
514 Redox properties of compost-derived organic matter and their association with
515 polarity and molecular weight. *Sci Total Environ,* 665**,** 920-928.
516 Jindo, K., Suto, K., Matsumoto, K., Garcia, C., Sonoki, T., & Sanchez-Monedero, M.
517 A., (2012) Chemical and biochemical characterisation of biochar-blended
518 composts prepared from poultry manure. *Bioresour Technol,* 110**,** 396-404.
519 Jones, D. L., Murphy, D. V., Khalid, M., Ahmad, W., Edwards-Jones, G., & DeLuca, T.
520 H., (2011) Short-term biochar-induced increase in soil CO2 release is both
521 biotically and abiotically mediated. *Soil Biology and Biochemistry,* 43**,**
522 1723-1731.

523 Katyal, J. C., & Sharma, B. D., (1991) DTPA-extractable and total Zn, Cu, Mn, and
524 Fe in Indian soils and their association with some soil properties. *Geoderma,* 49**,**
525 165-179.
526 Kim, H.S., Kim, K.R., Kim, H.J., Yoon, J.H., Yang, J. E., Ok, Y. S., Owens, G., & Kim,
527 K.H., (2015) Effect of biochar on heavy metal immobilization and uptake by
528 lettuce (Lactuca sativa L.) in agricultural soil. *Environmental Earth Sciences,* 74**,**
529 1249-1259.
530 Lasheen, M. R., & Ammar, N. S., (2016) Ex situ remediation technology for heavy
531 metals in contaminated sediment. *Desalination & Water Treatment,* 57**,** 827-834.
532 Lazzari, L., Sperni, L., Bertin, P., & Pavoni, B., (2000) Correlation between inorganic
533 (heavy metals) and organic (PCBs and PAHs) micropollutant concentrations
534 during sewage sludge composting processes. *Chemosphere,* 41**,** 430-435.
535 Li, L., Xu, Z., Wu, J., & Tian, G., (2010) Bioaccumulation of heavy metals in the
536 earthworm Eisenia fetida in relation to bioavailable metal concentrations in pig
537 manure. *Bioresour Technol,* 101**,** 3430-6.
538 Liang, B., Lehmann, J., Solomon, D., Kinyangi, J., Grossman, J., O'Neill, B.,
539 Skjemstad, J. O., Thies, J., Luizão, F. J., Petersen, J., & Neves, E. G., (2006)
540 Black Carbon Increases Cation Exchange Capacity in Soils. *Soil Science Society*
541 *of America Journal,* 70**,** 1719-1730.
542 Liang, J., Yang, Z., Tang, L., Zeng, G., Yu, M., Li, X., Wu, H., Qian, Y., Li, X., & Luo,
543 Y., (2017) Changes in heavy metal mobility and availability from contaminated

544 wetland soil remediated with combined biochar-compost. *Chemosphere,* 181**,**
545 281-288.
546 Liu, W., Huo, R., Xu, J., Liang, S., Li, J., Zhao, T., & Wang, S., (2017) Effects of
547 biochar on nitrogen transformation and heavy metals in sludge composting.
548 *Bioresour Technol,* 235**,** 43-49.
549 Liu, Y., Ma, L., Li, Y., & Zheng, L., (2007) Evolution of heavy metal speciation
550 during the aerobic composting process of sewage sludge. *Chemosphere,* 67**,**
551 1025-32.
552 Mayer, L. M., Schick, L. L., & Loder III, T. C., (1999) Dissolved protein fluorescence
553 in two Maine estuaries. *Marine Chemistry,* 64**,** 171-179.
554 Meng, X., Liu, B., Zhang, H., Wu, J., Yuan, X., & Cui, Z., (2019) Co-composting of
555 the biogas residues and spent mushroom substrate: Physicochemical properties
556 and maturity assessment. *Bioresour Technol,* 276**,** 281-287.
557 Paz-Ferreiro, J., Lu, H., Fu, S., Méndez, A., & Gascó, G., (2014) Use of
558 phytoremediation and biochar to remediate heavy metal polluted soils: a review.
559 *Solid Earth,* 5**,** 65-75.
560 Ranalli, G., Bottura, G., Taddei, P., Garavani, M., Marchetti, R., & Sorlini, C., (2001)
561 Composting of solid and sludge residues from agricultural and food industries.
562 Bioindicators of monitoring and compost maturity. *J Environ Sci Health A Tox*
563 *Hazard Subst Environ Eng,* 36**,** 415-36.
564 Rashad, F. M., Saleh, W. D., & Moselhy, M. A., (2010) Bioconversion of rice straw
565 and certain agro-industrial wastes to amendments for organic farming systems: 1.

566 Composting, quality, stability and maturity indices. *Bioresour Technol,* 101**,**
567 5952-60.
568 Ren, L. M., Li, G. X., Shen, Y. J., Schuchardt, F., & Lu, P., (2010) Chemical
569 precipitation for controlling nitrogen loss during composting. *Waste Manag Res,*
570 28**,** 385-94.
571 Riffaldi, R., Levi-Minzi, R., Pera, A., & Bertoldi, M. d., (1986) Evaluation of compost
572 maturity by means of chemical and microbial analyses. *Waste Management &*
573 *Research,* 4**,** 387-396.
574 Sanchez-Garcia, M., Alburquerque, J. A., Sanchez-Monedero, M. A., Roig, A., &
575 Cayuela, M. L., (2015) Biochar accelerates organic matter degradation and
576 enhances N mineralisation during composting of poultry manure without a
577 relevant impact on gas emissions. *Bioresour Technol,* 192**,** 272-9.
578 Serramia, N., Sanchez-Monedero, M. A., Fernandez-Hernandez, A., Civantos, C. G.,
579 & Roig, A., (2010) Contribution of the lignocellulosic fraction of two-phase
580 olive-mill wastes to the degradation and humification of the organic matter
581 during composting. *Waste Manag,* 30**,** 1939-47.
582 Singh, J., & Kalamdhad A. S., (2015) Influences of natural zeolite on speciation of
583 heavy metals during rotary drum composting of green waste. *Chemical*
584 *Speciation & Bioavailability,* 26**,** 65-75.
585 Singh, J., & Kalamdhad, A. S., (2013). Assessment of bioavailability and leachability
586 of heavy metals during rotary drum composting of green waste (water hyacinth).
587 *Ecological Engineering*, 52, 59-69.

588 Singh, W. R., Das, A., & Kalamdhad, A., (2012) Composting of Water Hyacinth using
589 a Pilot Scale Rotary Drum Composter. *Environmental Engineering Research,* 17**,**
590 69-75.
591 Tang, J., Zhuang, L., Yu, Z., Liu, X., Wang, Y., & Wen, P., et al. (2018). Insight into
592 complexation of cu(ii) to hyperthermophilic compost-derived humic acids by
593 eem-parafac combined with heterospectral two dimensional correlation analyses.
594 ence of The Total Environment, 656, 29-38.
595 Walter, I., Martinez, F., & Cala, V., (2006) Heavy metal speciation and phytotoxic
596 effects of three representative sewage sludges for agricultural uses. *Environ*
597 *Pollut,* 139**,** 507-14.
598 Wang D., Xing L., Xie J, et al (2010a). Application of advanced characterization
599 techniques to assess DOM treatability of micro-polluted and un-polluted
600 drinking source waters in China. *Chemosphere*, 81, 39-45.
601 Wang, S. Y., Tsai, M. H., Lo, S. F., & Tsai, M. J., (2008) Effects of manufacturing
602 conditions on the adsorption capacity of heavy metal ions by Makino bamboo
603 charcoal. *Bioresour Technol,* 99**,** 7027-33.
604 Wang, X., Chen, X., Liu, S., & Ge, X., (2010b). Effect of molecular weight of
605 dissolved organic matter on toxicity and bioavailability of copper to lettuce.
606 *Journal of Environmental ences*,12, 1960-1965.
607 Yao, X., Zhang, Y., Zhu, G., Qin, B., Feng, L., Cai, L., & Gao, G., (2011) Resolving
608 the variability of CDOM fluorescence to differentiate the sources and fate of
609 DOM in Lake Taihu and its tributaries. *Chemosphere,* 82**,** 145-55.

610 Yi, Y., Yang, Z., & Zhang, S., (2011) Ecological risk assessment of heavy metals in
611 sediment and human health risk assessment of heavy metals in fishes in the
612 middle and lower reaches of the Yangtze River basin. *Environ Pollut,* 159**,**
613 2575-85.
614 Yu, Z., Tang, J., Liao, H., Liu, X., Zhou, P., Chen, Z., Rensing, C., & Zhou, S., (2018)
615 The distinctive microbial community improves composting efficiency in a
616 full-scale hyperthermophilic composting plant. *Bioresour Technol,* 265**,** 146-154.
617 Yuan, Y., Xi, B., He, X., Tan, W., Gao, R., Zhang, H., Yang, C., Zhao, X., Huang, C.,
618 & Li, D., (2017) Compost-derived humic acids as regulators for reductive
619 degradation of nitrobenzene. *J Hazard Mater,* 339**,** 378-384.
620 Zeng, G. M., Huang, H. L., Huang, D. L., Yuan, X. Z., Jiang, R. Q., Yu, M., Yu, H. Y.,
621 Zhang, J. C., Wang, R. Y., & Liu, X. L., (2009) Effect of inoculating white-rot
622 fungus during different phases on the compost maturity of agricultural wastes.
623 *Process Biochem,* 44**,** 396-400.
624 Zhang, D., Luo, W., Li, Y., Wang, G., & Li, G., (2018) Performance of co-composting
625 sewage sludge and organic fraction of municipal solid waste at different
626 proportions. *Bioresour Technol,* 250**,** 853-859.
627 Zhang, J., Chen, G., Sun, H., Zhou, S., & Zou, G., (2016) Straw biochar hastens
628 organic matter degradation and produces nutrient-rich compost. *Bioresour*
629 *Technol,* 200**,** 876-83.
630 Zhang, L. & Sun, X., (2017) Addition of fish pond sediment and rock phosphate
631 enhances the composting of green waste. *Bioresour Technol,* 233**,** 116-126.

632 Zhao, X., He, X., Xi, B., Gao, R., Tan, W., Zhang, H., Huang, C., Li, D., & Li, M.,
633 (2017) Response of humic-reducing microorganisms to the redox properties of
634 humic substance during composting. *Waste Manag,* 70**,** 37-44.
635 Zhao, X., Li, B., Ni, J., & Xie, D., (2016) Effect of four crop straws on transformation
636 of organic matter during sewage sludge composting. *Journal of Integrative*
637 *Agriculture,* 15**,** 232-240.
638 Zhou, H., Meng, H., Zhao, L., Shen, Y., Hou, Y., Cheng, H., & Song, L., (2018) Effect
639 of biochar and humic acid on the copper, lead, and cadmium passivation during
640 composting. *Bioresour Technol,* 258**,** 279-286.
641 Zorpas, A. A., Constantinides, T., Vlyssides, A. G., Haralambous, I., & Loizidou, M.,
642 (2000) Heavy metal uptake by natural zeolite and metals partitioning in sewage
643 sludge compost. *Bioresource Technology,* 72(2)**,**113-119.

Figures

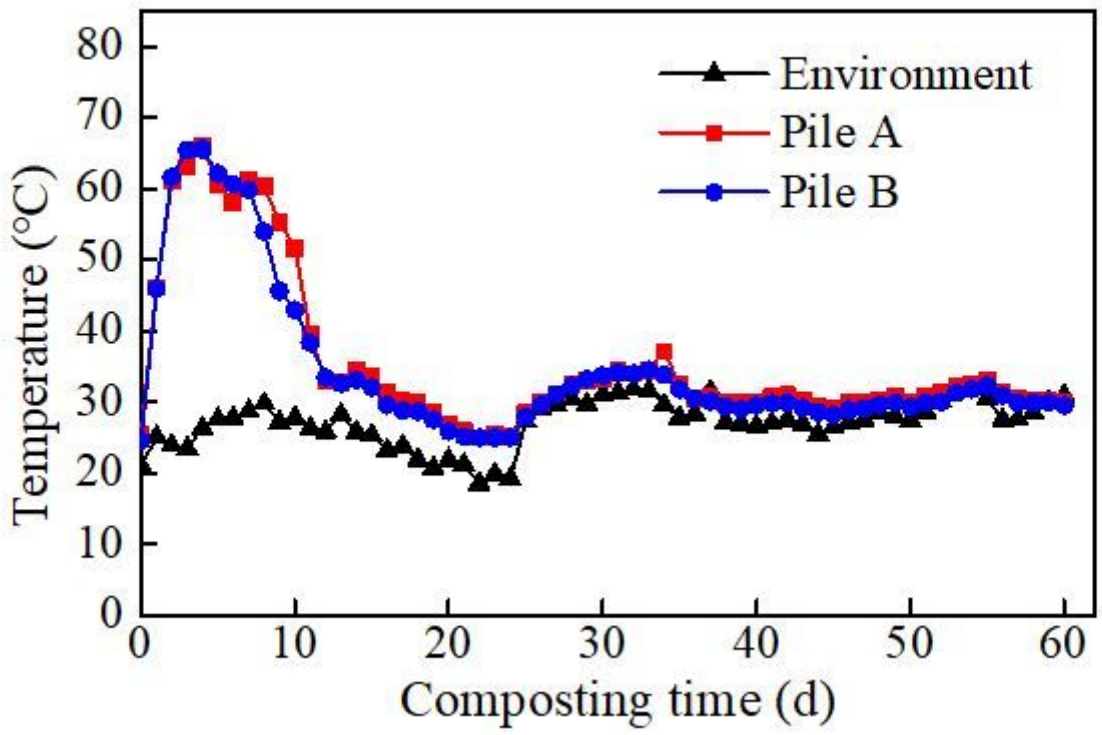

Figure 1

The temperature diagram during composting process.

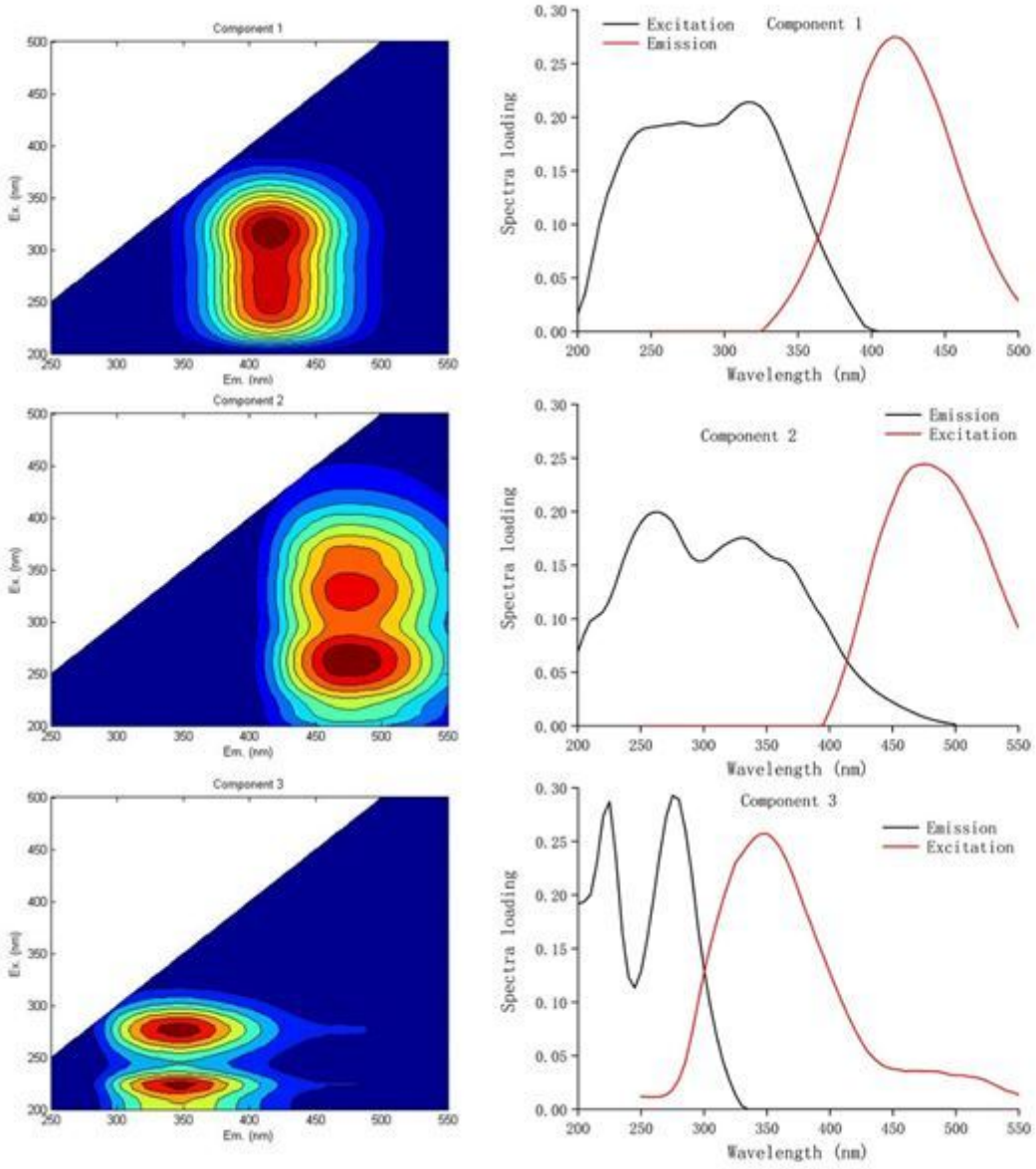

Figure 2

Three fluorescent components identified by PARAFAC model and their loadings.

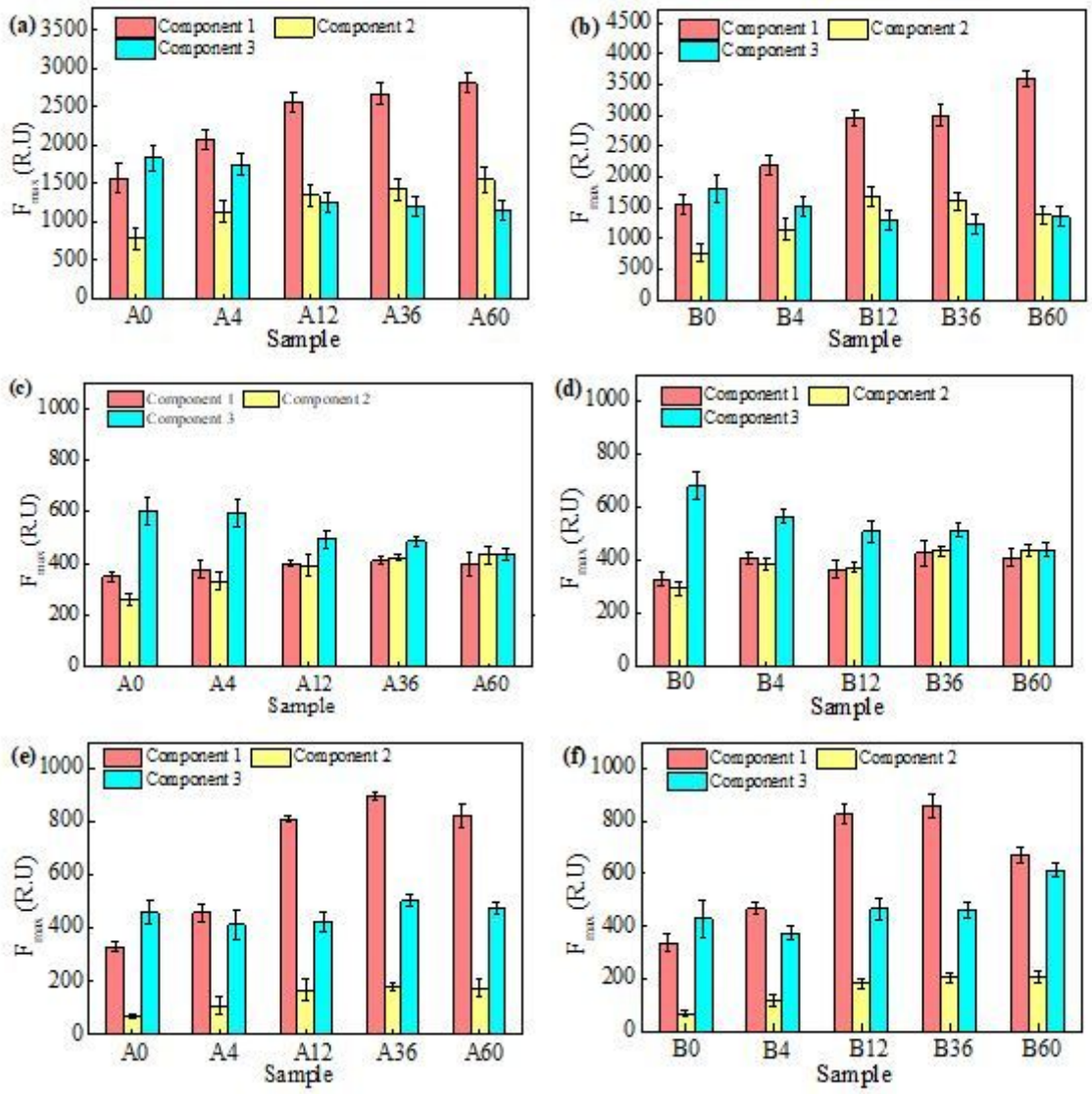

Figure 3

The evolution of the Fmax of different fluorescent components of FA (a, b), HA (c, d) and HyI (e, f) during composting. A0, A4, A12, A36, and A60 respected day 0, 4, 12, 36, and 60 of pile A, respectively; B0, B4, B12, B36, and B60 respected day 0, 4, 12, 36, and 60 of pile B, respectively.

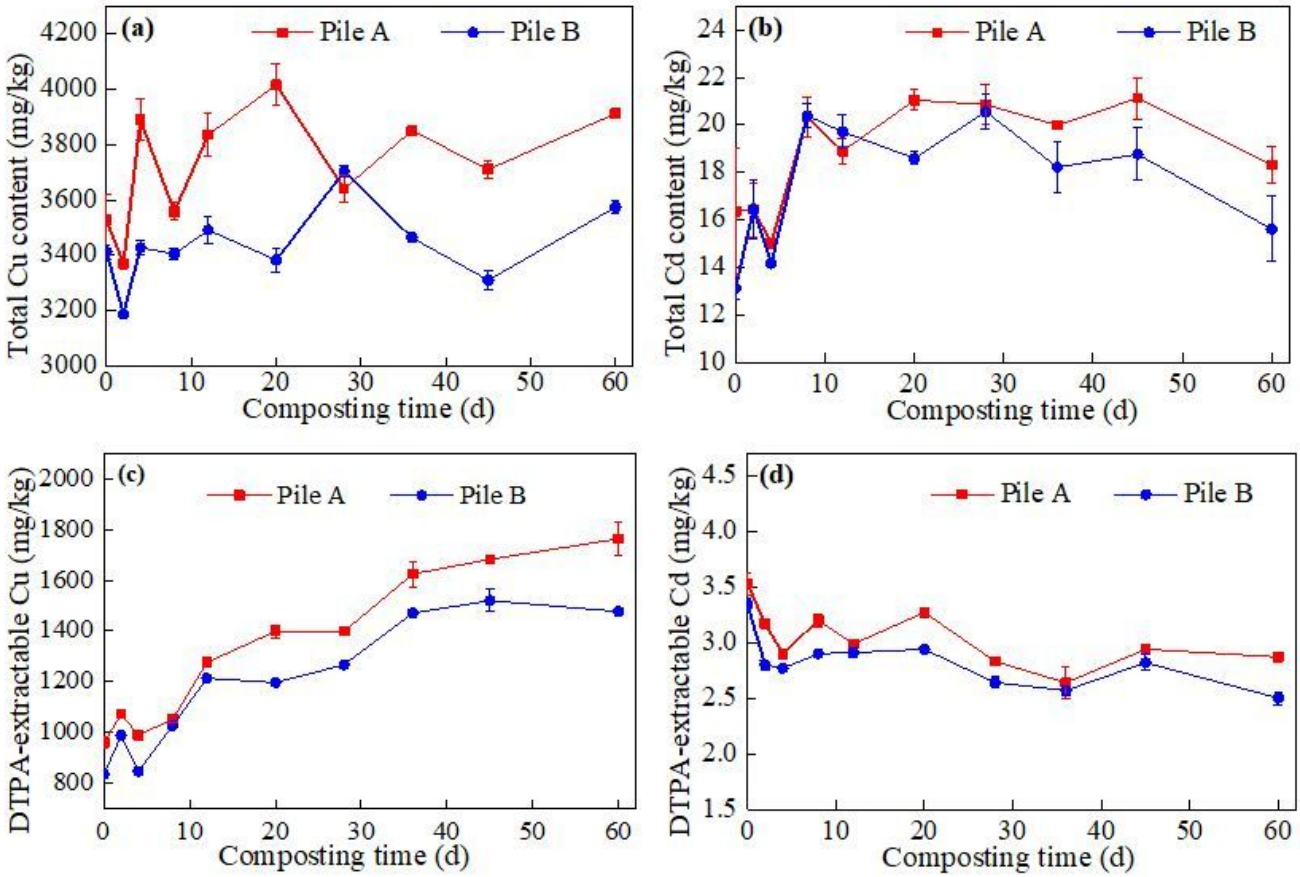

Figure 4

Changes in contents of total Cu and Cd (a, b), DTPA-extractable Cu and Cd (c, d) during composting process.

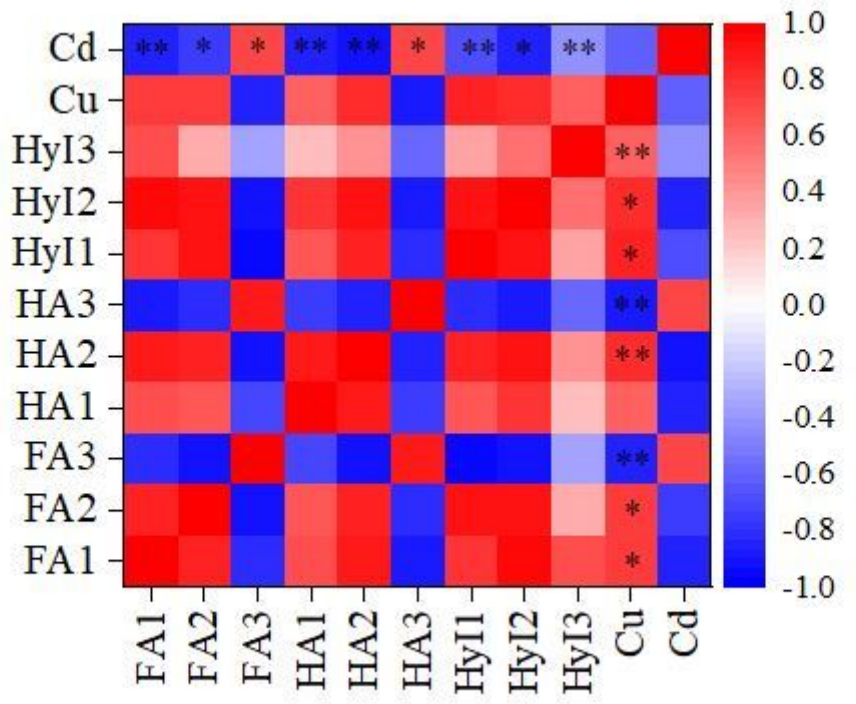

Figure 5

The diagram of the relationship between the fluorescent components of FA, HA, and HyI and the DTPA-extractable Cu and Cd contents during the compost process. FA1, FA2, FA3, HA1, HA2, HA3, HyI1, HyI2, and HyI3 respected the C1, C2, C3 of the FA, the C1, C2, C3 of the HA, and C1, C2, C3 of the HyI, respectively. **, Significant correlation at.01 level (bilateral). *, Significant correlation at the 0.05 level (bilateral).